IEEE Photonics Journal
An IEEE Photonics Society Publication

Open Access

Adaptive Single-Mode Fiber Coupling Method Based on Coarse-Fine Laser Nutation

Volume 10, Number 6, December 2018

Bo Li
Yutong Liu
Shoufeng Tong
Lei Zhang
Haifeng Yao

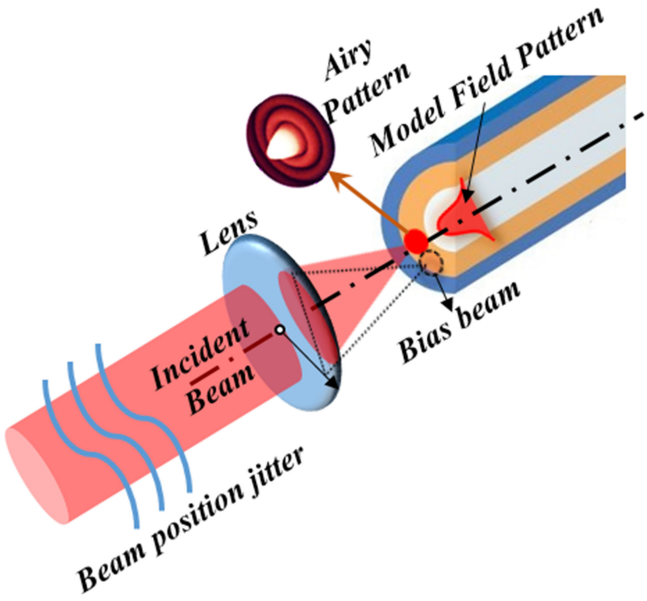

DOI: 10.1109/JPHOT.2018.2877212
1943-0655 © 2018 IEEE

IEEE photonics SOCIETY
IEEE

Adaptive Single-Mode Fiber Coupling Method Based on Coarse-Fine Laser Nutation

Bo Li,[1] **Yutong Liu**,[2] **Shoufeng Tong**,[3] **Lei Zhang**,[3] **and Haifeng Yao**[1]

[1]Institute of Photoelectric Engineering, Changchun University of Science and Technology, Changchun 130022, China
[2]College of Optical and Electronical Information, Changchun 130114, China
[3]Institute of Space Photoelectric Technology, Changchun University of Science and Technology, Changchun 130022, China

DOI:10.1109/JPHOT.2018.2877212

Manuscript received August 7, 2018; revised October 11, 2018; accepted October 16, 2018. Date of publication October 22, 2018; date of current version December 5, 2018. Corresponding author: Shoufeng Tong (e-mail: dsphd2017@126.com).

Abstract: One of the major restrictions of the free-space optical communication systems is the limitation of single-mode fiber (SMF) coupling efficiency that impacts the system performance. In this paper, an adaptive coupling method for optical communication system based on coarse-fine laser nutation technique was presented. The scanning strategy and algorithm were set up and experimentally examined. The experimental results demonstrate that the coarse-fine laser nutation technique is capable of achieving a good coupling efficiency even the beam spot and the SMF do not coincide with each other at the start. The SMF center calculation accuracy of coarse and fine scanning stage were 0.25 and 0.01 μm, respectively. And the average coupling efficiency of the system can increase from 0.351 in open loop to 0.624 in closed loop under a simulated atmospheric turbulence condition, the offset compensation error was 0.1245 μm when turbulence induced. Finally, some factors influencing the systems were also discussed.

Index Terms: Free space optical communication, single-mode fiber coupling, coarse-fine laser nutation, offset compensation.

1. Introduction

Compared to the traditional microwave communication system, the free space optical communication technique between ground and satellite offers several significant advantages of small size, low power consumption, high confidentiality, high security and high data rate.[1]–[5]. In this system, coupling the received space light into a single-mode fiber (SMF) is a key process, especially for deep-space laser communication applications which operated in a photon-starve link. In addition, the coupling efficiency is always unstable and easy to be degraded because of the random radial offsets between SMF and optical beam which induced by atmospheric turbulence, platform vibration and fiber static angular misalignment [6]–[8]. Thus, active single-mode fiber coupling methods have attracted attentions for higher and constant coupling efficiency in recent years.

In this regard, up to now, several solutions have been suggested to achieve highly efficient coupling. In [9] a fiber nutation method with simple structure was firstly proposed by Swanson,

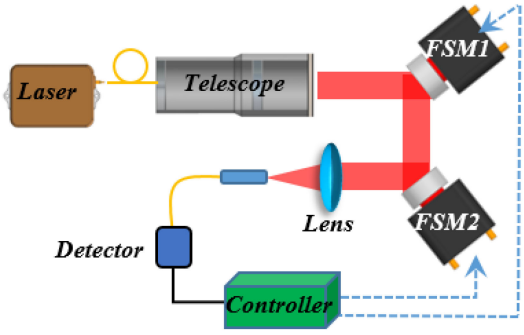

Fig. 1. Coarse-fine laser nutation system.

and the efficiency was 63% with 1 KHz respond speed. In [10] Thomas Weyrauch proposed an adaptive optical fiber coupling system which comprised of micro-electro mechanical deformable mirror and a VLSI gradient descent controller based on Adaptive Optics theory, it achieved 60% coupling efficiency. But due to the stochastic parallel gradient descent (SPGD) algorithm, the work bandwidth was low. In [11] another auto-coupling method using piezoelectric ceramics and five-point tracking arithmetic was proposed, but the algorithm was complex and it failed to compensate the bias at a high frequency. In [12] a fast-steering mirror that can operate at high frequencies under atmospheric turbulence was fabricated to increase fiber-coupling efficiency, but the two sub-optical paths structure was complex and easy to introduce artificial errors. In [13] a new adaptive-optic device named adaptive fiber coupler (AFC), which could compensate angular jitters and improve the SMF coupling efficiency in some degree, was verified. But the control bandwidth is only about 20 Hz under atmospheric turbulence. In [14] a fiber-coupling method based on laser nutation was demonstrated and the efficiency was improved by 6.5% to 73.5% when vibration induced. But the experiment was carried out on condition that the beam had already aligned with the SMF in advance. In [15], a similar method was proposed by using piezo scanner tube.

All the previous works only focused on the situation that the beam has already coincided with SMF partially. But in real application, due to the violent vibration, it can happen that the beam completely deviates from SMF. This will result the system invalidation. In this paper, an improved laser nutation scanning strategy and algorithm which based on coarse-fine acquisition was presented. The adaptive coupling system will not only solve the coupling problem at small radial offsets, but also put forward a method for fast acquisition and tracking when there exists large deviations between beam and SMF. The method can improve and keep the SM average coupling efficiency at a steady value. The paper is organized as follows. In Section 2, we give the structure of the coarse-fine laser nutation system and briefly introduce the working principle of the method. The detailed closed-loop nutation algorithm and correction process are presented in Section 3. An experiment is conducted in Section 4 to verify the coupling ability of the proposed method. In Section 5, the influences of wave-front distortion, beams size and nutation amplitude on the nutation system are discussed. Finally, conclusions are drawn in Section 6.

2. System Structure and Working Principle

The structure of the adaptive SM coupling system based on the coarse-fine laser nutation technique is shown in Fig. 1. It consists of a 1550 nm laser, a telescope, two fast-steering mirrors, a focusing lens, an APD detector and a servo controller.

When the system works, the collimated laser beam will be sent to a radial offset compensation fast-steering mirror (FSM1), and then reflected to nutation scanning FSM2, then the beam will be focused by the focusing lens and coupled into a SMF. An APD detector is located behind the tail of SMF to detect the coupled optical power. The radial offsets calculation and fiber core's coordinates calculation will be done by the controller according to the detected optical power, and then outputs signals to FSM1 for offsets compensation and FSM2 for nutation scanning optimization

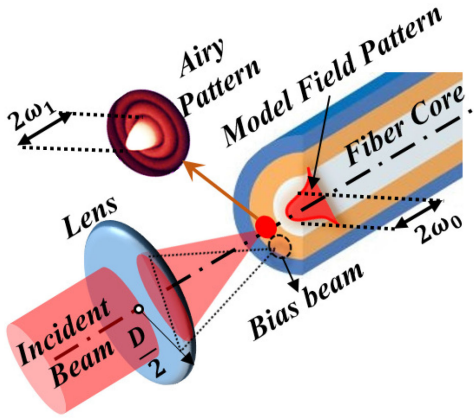

Fig. 2. Schematic illustration of the SMF coupling.

and adjustment. Finally, a high and stable coupling efficiency will be achieved with radial offsets vibration.

3. Laser Nutation Scanning Strategy and Algorithm

Firstly, the basic principle of coupling is needed to be introduced briefly. When the incident beam is ideal, the distribution of the laser beam which focused by a lens with diameter D and focal length f on the fiber end becomes an Airy pattern, just as is shown in Fig. 1. Then the spatial light to SMF coupling efficiency can be expressed as [16]

$$\eta = \frac{\left|\int A(r)M(r)dr\right|}{\int |A(r)|^2 dr} \tag{1}$$

The phase term A(r) and the amplitude of the Gaussian distribution M(r) can be expressed by

$$A(r) = \frac{\pi D^2}{4\lambda f}\left[2\frac{J_1(3.83/\omega_1)}{3.83r/\omega_1}\right] \tag{2}$$

$$M(r) = \sqrt{\frac{2}{\pi\omega_0^2}}\exp\left(-\frac{r^2}{\omega_0^2}\right) \tag{3}$$

where λ is the optical wavelength, r is the radial offset on the focal plane, $J_1(\cdot)$ is the Bessel function of the first kind of order zero, ω_1 is the Airy disk radius, ω_0 is the mode field radius of SMF. However, in the practical optical communications, the laser beam position will jitter randomly due to the unstable atmospheric turbulence channel. If there is an offset bias ρ between the center of the focused beam and the normal axis of the fiber core, the coupling efficiency η can be given after a series of mathematical derivation [14]

$$\eta\left(\frac{\rho}{\omega_0}\right) = \frac{2\pi}{1+2(\rho/\omega_0)^2}\cdot\exp\left[-2\cdot\frac{3.83^2}{8}\cdot\frac{1+2(\rho/\omega_0)^2}{(\omega_1/\omega_0)^2}\right]I_{1/2}^2\left[\frac{3.83^2}{8}\cdot\frac{1+2(\rho/\omega_0)^2}{(\omega_1/\omega_0)^2}\right] \tag{4}$$

where I_x is the Modified Bessel Function. According to the equation (4), we can know that the maximum coupling efficiency is $\eta = 81.45\%$ with a $1.711\omega_0$ Airy disk radius and without any deviation between the light spot and fiber core. However, the coupling efficiency will degrade severely with the increasing of offset bias ρ, as shown in Fig. 3. Therefore, it's necessary to compensate the radial offset bias to improve the SMF coupling efficiency as well as the optical communication system performance.

Firstly, we concentrate on the circumstance that there is no overlapping area between the beam spot and the SMF. Under the assumption that the laser spot radius is $1.711\omega_0$ and the initial nutation

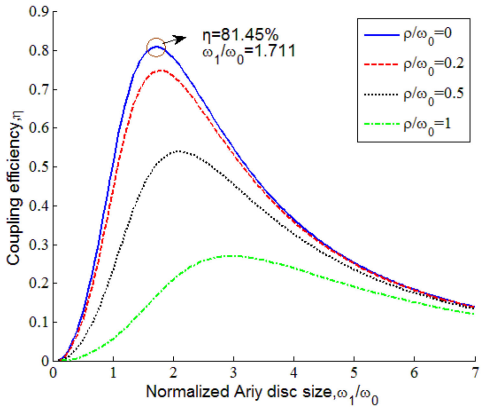

Fig. 3. SMF coupling efficiency as a function of normalized Airy disk radius with different radial biases.

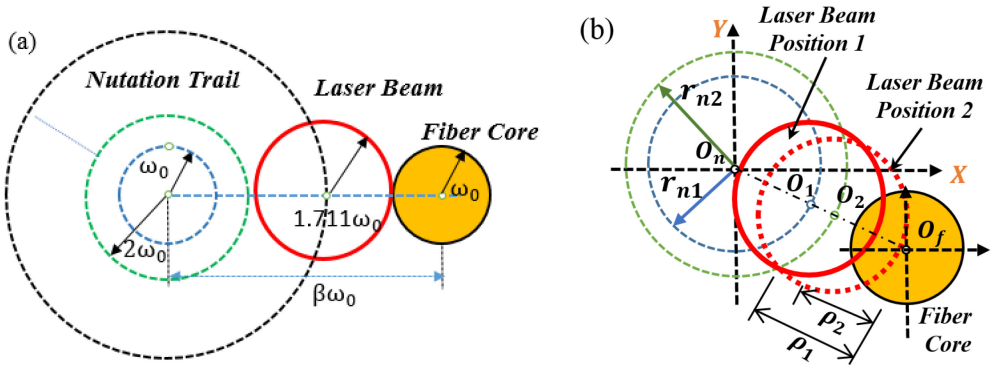

Fig. 4. Coarse scanning illustration. (a) nutation amplitude feed rate; (b) relative position in two adjacent periods.

amplitude is $r_n = \omega_0$, two scenarios can occur at the initial stage: a) the initial radial offset is larger than $1.711\omega_0$, in this case, there will have no or discontinuous output of detector during the first nutation scanning cycle; b) the initial radial offset is less than $1.711\omega_0$ and the detector will have continuous output. Thus, a comprehensive scanning strategy needs to be put forward.

Fig. 4 shows the first scenario and corresponding coarse scanning strategy. Assuming that the initial radial offset between nutation center and fiber core is $\beta\omega_0$, and the initial nutation amplitude is ω_0. When the system begins to work, the laser beam moves along the blue dotted line, and it's obvious that the beam cannot coincide with the fiber during the whole cycle. Increasing the scanning amplitude r_n at a feed rate $\Delta r_1 = \omega_0$ until $r_n \geq (\beta - 2.711)\omega_0$, then the beam spot overlaps with SMF for the first time, the coupled optical power will be detected firstly by the APD, as depicted in Fig. 4(a). We should note that there is only one maximum power value in each cycle according to the symmetry of circle motion. After that, as shown in Fig. 4(b), a new feed rate $\Delta r_2 = \omega_0/n$ (n is a integer) induced and both the max power values P_{max1}, P_{max2} and the nutation amplitudes r_{n1}, r_{n2} are obtained in two adjacent periods. In the Cartesian coordinate system, O_n is the nutation center, O_1 and O_2 are the center of spot at position 1 and position 2, respectively. Assuming that the position of SMF is fixed at O_f and the power of incident light is considered as a constant P_{in} during the whole scanning process, according to Eq. 4, the radial offsets ρ_x (x = 1, 2) can be calculated by

$$P_{max1}/P_{in} = \eta(\rho_1/\omega_0) \tag{5a}$$

$$P_{max2}/P_{in} = \eta(\rho_2/\omega_0) \tag{5b}$$

$$\rho_1 - \rho_2 = r_{n2} - r_{n1} = \Delta r_2 \tag{5c}$$

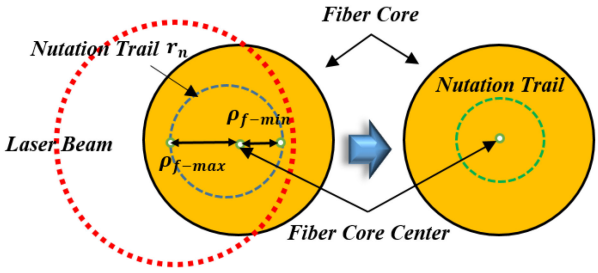

Fig. 5. Principle of fine nutation scanning principle.

Then the coordinate position (x_f, y_f) of fiber core can be obtained after N scans by

$$x_f = \frac{x_1 + \cdots + x_n}{N} = \frac{(r_1 + \rho_1)\cos\omega t_1 + \cdots + (r_n + \rho_n)\cos\omega t_n}{N}$$
$$y_f = \frac{y_1 + \cdots + y_n}{N} = \frac{(r_1 + \rho_1)\sin\omega t_1 + \cdots + (r_n + \rho_n)\sin\omega t_n}{N} \quad (6)$$

where ω stands for nutation scanning angular speed. Then the offset between nutation center and fiber core can be compensated by FSM1 according to the calculated coordinates. But to save the time of coarse stage, the sampling frequency and sampling points are limited, this will result in relatively large calculation errors. So, a fine scanning procedure is indispensable.

Fig. 5 depicts the fine nutation stage, the blue dotted line is the nutation trail of laser beam, and r_n is the nutation amplitude. During this stage, the detector can get one maximum power P_{f-max} and one minimum power P_{f-min} during each cycle. Solve the below equations [15], we can get the offsets.

$$P_{f-max}/P_{f-in} = \eta(\rho_{f-min}/\omega_0) \quad (7a)$$
$$P_{f-min}/P_{f-in} = \eta(\rho_{f-max}/\omega_0) \quad (7b)$$
$$\rho_{f-max} + \rho_{f-min} = 2r_n \quad (7c)$$
$$x_f = \frac{x_1 + \cdots + x_n}{n} = \frac{\sum_1^N (\rho_{f-max} - r_f)\cos\omega t_n}{N}$$
$$y_f = \frac{y_1 + \cdots + y_n}{n} = \frac{\sum_1^N (r_f - \rho_{f-min})\sin\omega t_n}{N} \quad (7d)$$

When the offsets are compensated by FSM1, the beam spot will move along the green dotted line. And the overlapping area between the spot and the fiber as well as the output of APD is constant. The algorithm flow chart is shown in Fig. 6.

The main purpose of the coarse-fine laser nutation system is to compensate the radial offset bias, but take another look, the system also can be regarded as a method of utilizing the random radial jitters to compensate the nutation amplitudes adaptively. Based on this, an appropriate signal will be applied to FSM2 finally to ensure a suitable nutation amplitude for a high and stable coupling efficiency. However, it must to be noted that the real incident power P_{in} is not constant because of the unstable atmospheric turbulence channel, this will lead to the coordinate calculation errors.

4. Experimental Results and Discussion

It should be noted that, in FSO system, Adaptive Optics (AO) system and Pointing, Acquisition, and Tracking (PAT) system are needed to correct the atmospheric turbulence aberration and improve

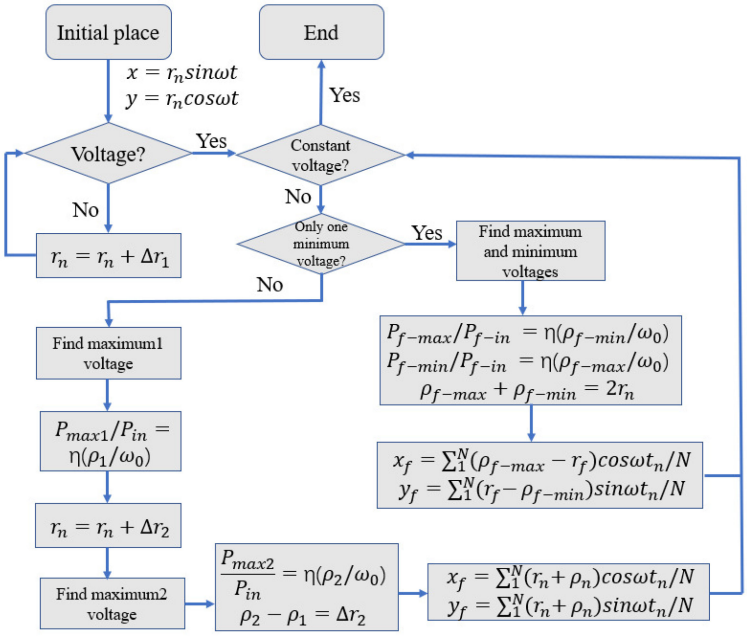

Fig. 6. The laser nutation algorithm flow chart.

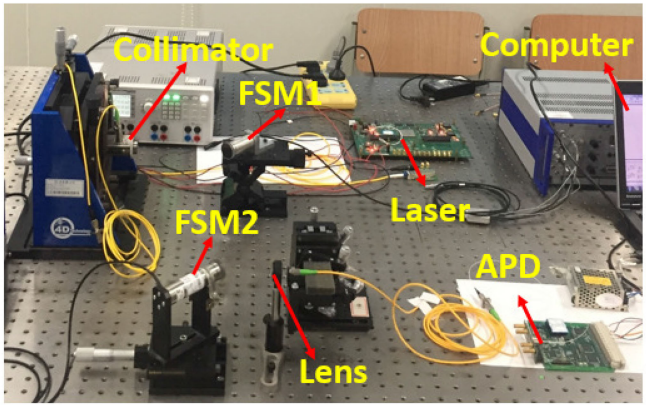

Fig. 7. The experimental system of coarse-fine laser nutation scanning.

the tracking accuracy between satellite and ground station. Therefore, the coupling system will be located behind these sub-systems.

The SMF coupling method based on coarse-fine laser nutation was experimentally examined in laboratory. As shown in Fig. 7, a 10 mW laser beam with the wavelength of 1550 nm was collimated and sent to an offset compensation FSM1 and a nutation FSM2, the beam focused by a focus lens and coupled into a 9 μm mode-field diameter SMF which was fixed on a 6D adjusting mount. A pigtailed APD was located at the end of SMF to detect coupled optical power. The maximum power coupled into SMF was 6.56 mW after a series of manual adjustment. Therefore, we can conclude that the maximum SMF coupling efficiency in this system was about 65.6%. The manufacturers and models of the instruments we used are listed in Table 1.

The position of focused beam center was taken to be the origin of the coordinate system, then we adjusted the fiber position to coordinate point (13 μm, 13 μm), ($-$14 μm, 14 μm), ($-$15 μm, $-$15 μm) and (16 μm, $-$16 μm) to ensure that the beam spot completely deviates from the SMF. A nutation signal with 20 μm amplitude was applied to FSM2, then the efficiencies were obtained

TABLE 1
Experiment Instruments Information

Instrument	Manufacturer	Model
Laser	Linktel	LX1733CDA
Collimator	THORLABS	RC08FC-P01
FSM	PI	S-330.8SL
APD	VOXTEL	RUC1-JITC
Lense	THORLABS	C280TMD-C, f=18.4mm, d=5.5mm

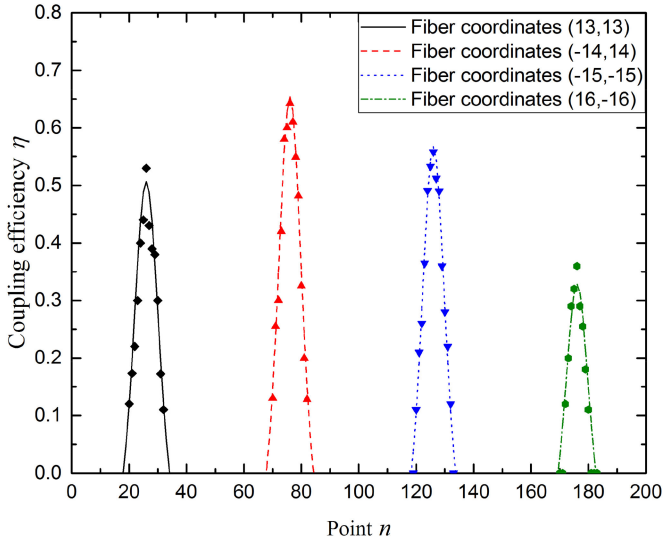

Fig. 8. Measured coupling efficiency values in coarse-scanning stage.

TABLE 2
Calculation Results With Different Feed Rates in Coarse-Scanning Stage

Coordinate of SMF	Feed Rate Δr=0.1μm	Feed Rate Δr=0.5μm	Feed Rate Δr=1μm
(13,13)	(12.7415,12.7471)	(12.7514,13.7523)	(12.7608,12.7612)
(-14,14)	(13.7455,13.7457)	(13.7525,13.7537)	(13.7614,13.7617)
(-15,-15)	(14.7453,14.7448)	(14.7507,14.7518)	(14.7620,14.7619)
(16,-16)	(15.7394,16.2425)	(15.7428,15.7476)	(15.7601,15.7528)
Accuracy	~0.25μm	~0.25μm	~0.24μm

after 200 times data acquisition, as depicted in Fig. 8. Only 52 data points have been obtained during the overlapping stage. The lines in Fig. 7 stand the theoretical coupling efficiency curves of different coordinates It can be seen that the experimental data and theory data are compatible basically.

Experiments of coarse-scanning calculation accuracy was demonstrated with nutation amplitude 20 μm. Table 2 shows the calculation results of SMF center coordinates by different feed rates 0.1 μm, 0.5 μm and 1 μm. The accuracy of coarse-scanning stage was relatively lower due to the lack of adequate data. The accuracy was about 0.25 μm at $\Delta r = 0.1$ μm and $\Delta r = 0.5$ μm, and it increased slightly to 0.24 μm when the feed rate was 1 μm.

Fig. 9 shows the measured values of fine scanning stage with amplitude $r = 1$ μm, $r = 2.5$ μm and $r = 3$ μm. We obtained 250 groups of data for each amplitude, though most of them were

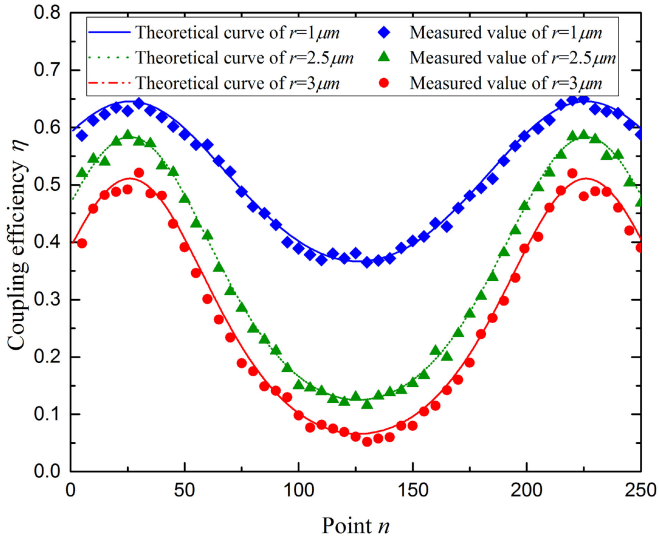

Fig. 9. Measured coupling efficiency values with amplitude r = 1 μm, r = 2.5 μm and r = 3 μm.

TABLE 3
Calculation Results of SMF Center With Different Amplitudes in Fine-Scanning Stage

Coordinate of SMF	Amplitude r=1μm	Amplitude r=2.5μm	Amplitude r=3μm
(1,1)	(0.9338,0.9341)	(0.9740,0.9740)	(0.9821,0.9925)
(1,1.5)	(0.9337,1.4336)	(0.9751,1.4745)	(0.9817,1.4812)
(-1.5,2)	(-0.9438,1.9343)	(-0.9744,1.9746)	(-1.5120,1.9901)
(-2,2.5)	(-1.9244,2.4381)	(-1.9748,2.4684)	(-1.9914,2.4867)
(-2.5, -3)	(-2.5723,-2.9459)	(-2.5255,-2.9767)	(-2.4885,-2.9897)
(-3,-3.5)	(-2.9355,-3.4262)	(-2.9737,-3.5281)	(-2.9915,-3.4923)
(-4,-4)	(-3.9466,-3.9371)	(-3.9724,-3.9692)	(-3.9837,-3.9934)
Accuracy	~0.07μm	~0.025μm	~0.01μm

lower than theoretical values but all the data basically agreed with theoretical curves. Then, we calculated the coordinates of SMF center, and the calculation accuracy is about 0.01 μm, which can be concluded from Table 3.

Here, experiment of SMF coupling efficiency with simulated turbulence induced by air conditioner was investigated. Fig. 10 shows the results of coupling efficiency in open and closed loop. The red line with triangle marks stands for an average efficiency of 0.52 with a nutation amplitude r = 2.4 μm under non-turbulence circumstance. The blue curve with diamond marks and the green curve with circle marks stand for the efficiency of open loop and closed loop in turbulence, respectively. It can be seen that the coupling efficiency was steady without turbulence, and it degraded severely when the turbulence induced. After the compensation, the average efficiency increased from 0.351 in open loop to 0.624 in closed loop. Fig. 11 shows the coupling efficiency errors under simulated atmospheric turbulence, the average error of coupling efficiency was 0.656–0.624 = 0.0356. It should be noted that due to the unstable incident light caused by turbulence,

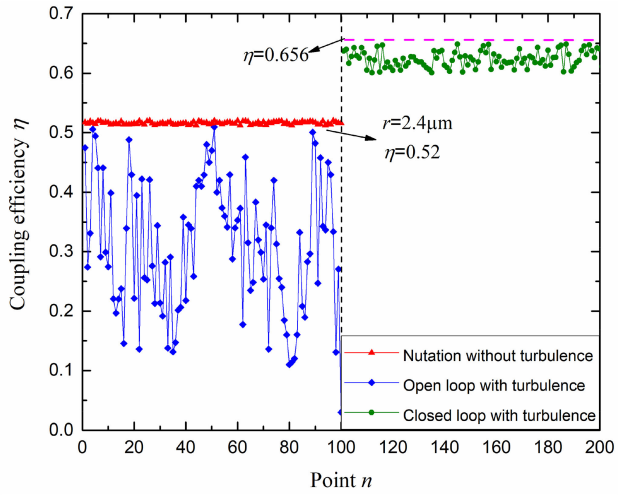

Fig. 10. Coupling efficiency in open and closed loop with turbulence.

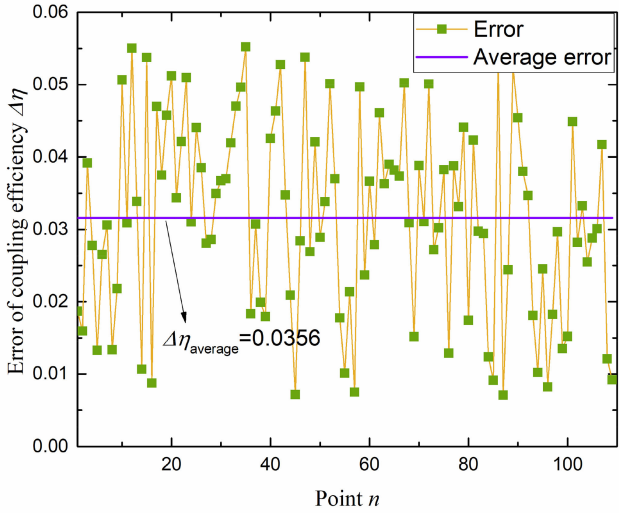

Fig. 11. Coupling efficiency errors with turbulence.

the average coordinate calculation error was (0.08803 μm, 0.08805 μm) which was larger than the experiment results without turbulence, the corresponding average radial offset compensation error was about 0.1245 μm. The correction bandwidth of the whole system was 100 Hz, which similar to the atmospheric frequency variation.

5. Analysis of Performance Affecting Factors

5.1 The Influence of Aberrations

The atmospheric turbulence channel is one of key factors hindering the performance of the optical communication system, and it results in distortion to the signal beam because the phase of the beam is randomly varied over the propagation path. According to [17], the coupling efficiency can be evaluated in the pupil plane A, which leads to

$$\langle \eta \rangle = \frac{\left\langle E_{\Phi}(r,\theta)\left|F_A(r)\right\rangle^2\right.}{\left\|E_{\Phi}(r,\theta)\right\|^2 \cdot \left\|F_A(r)\right\|^2} = \frac{\left\langle E_{\Phi}(r,\theta)\left|F_A(r)\right\rangle^2\right.}{\pi R^2(1-\varepsilon^2)} \tag{8}$$

TABLE 4
The Distorted Phase for Weighted Pupils With $\beta = 1.12$ and Different ε

β	ε	Tilt	Defocus	Astigmatism	Coma	Spherical aberration
1.12	0	$2.2414\pi a_i\rho$	$\pi a_i(4.1568\rho^2\text{-}1.6548)$	$2.3756\pi a_i\rho^2$	$\pi a_i(6.3228\rho^3\text{-}3.74\rho)$	$\pi a_i(12.4068\rho^4\text{-}11.3654\rho^2\text{+}1.601)$
1.12	0.15	$2.1986\pi a_i\rho$	$\pi a_i(4.2452\rho^2\text{-}1.7566)$	$2.332\pi a_i\rho^2$	$\pi a_i(6.2116\rho^3\text{-}3.6838\rho)$	$\pi a_i(12.966\rho^4\text{-}12.218\rho^2\text{+}1.8764)$
1.12	0.5	$1.878\pi a_i\rho$	$\pi a_i(5.4512\rho^2\text{-}3.091)$	$1.9076\pi a_i\rho^2$	$\pi a_i(6.327\rho^3\text{-}4.0884\rho)$	$\pi a_i(21.7392\rho^4\text{-}26.1492\rho^2\text{+}6.8624)$

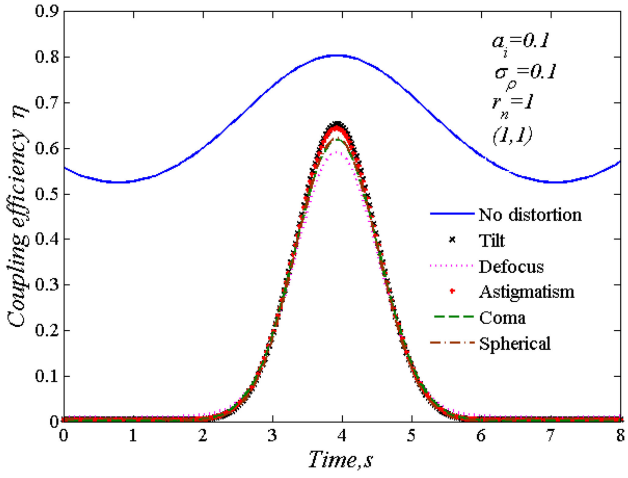

Fig. 12. Coupling efficiency of nutation scanning under different aberrations in the fine scanning stage.

where R is the radius of focus lens, ε is a linear central obstruction of the Cassegrain optical system, $E_\Phi(r, \theta)$ and $F_A(r)$ donate the distorted optical field and the backpropagated fiber mode, respectively. When there is a radial offset deviation ρ between the beam spot and the SMF, the coupling efficiency can be expressed as equation (9) after a series of analysis and formula

$$\langle\eta\rangle = \frac{8\beta^2}{1-\varepsilon^2}\left|\int_\varepsilon^1 \exp\left[j\varphi(\xi) - \beta^2\xi^2\left(1+2\frac{\sigma_\rho^2}{\omega_0^2}\right)\right] J_0\left(2\frac{\xi}{\omega_0}\beta\xi\right)\xi d\xi\right|^2 \tag{9}$$

where $\beta = R/\omega_a$, $\xi = r/R$ is the normalized radial distance, σ_ρ^2 is the variance of ρ, $J_0(\cdot)$ is the Bessel function, $\varphi(\xi)$ is the distorted phase.

The Zernike polynomials is widely used to expanded distorted phase, but research shows that Zernike expansion coefficients are no longer the best correction amplitudes in fiber coupling systems [18]. Fang Zhao, etc. presented a set of polynomials which are orthonormal over the pupil weighted by backpropagated fiber mode, then the distorted phase can be expressed as equation (10), where a_i is the distortion amplitude with unit λ. And the distorted phase for weighted pupils with $\beta = 1.12$ and different ε are listed in Table 4.

$$\Phi(r, \theta) = \sum_{i=1}^{J} 2\pi a_i G_i\left(\frac{r}{R}, \theta, \varepsilon, \beta\right) \tag{10}$$

The simulated curves of coupling efficiency with aberrations were obtained as shown in Fig. 12. The distortion amplitude is $a_i = 0.1$, the variance of radial offset deviation is $\sigma_\rho^2 = 0.01$, the nutation amplitude is $r_n = 1\ \mu$m, the coordinate of SMF core is (1 μm, 1 μm) and the beam radius is $\omega_a = 1.711\omega_0$. It can be seen that the coupling efficiency declines drastically when the aberrations induced. The trend of curves of aberrations are similar to each other, but the coupling efficiency

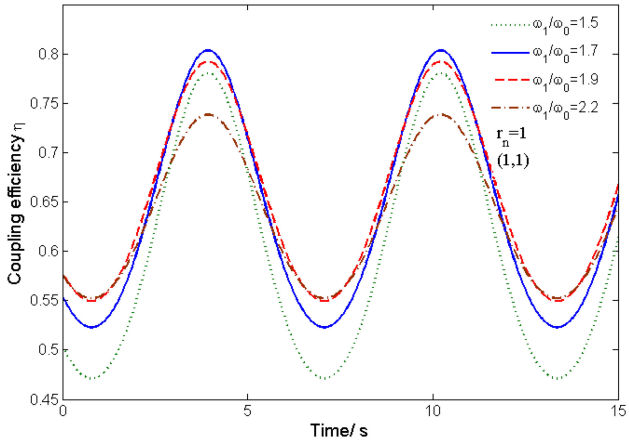

Fig. 13. Coupling efficiency of nutation scanning with different radius radios in the fine scanning stage.

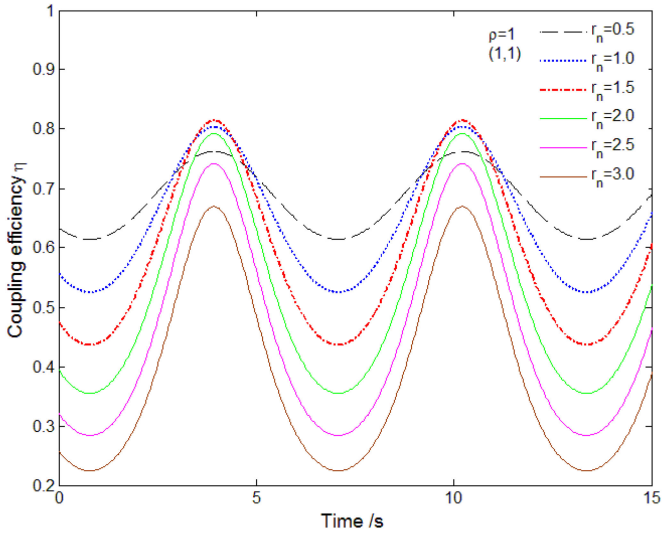

Fig. 14. Coupling efficiency of nutation scanning with different radius radios in the fine scanning stage.

loss caused by defocus is much more than the others. However, compared to the ideal blue line, the large slopes of distorted curves indicate that there will be benefit for calculation accuracy of SMF core, because the data values collected in the same cycle differ more greatly from each other than the data obtained from the ideal condition.

5.2 The Influence of Beam Radius

It is obvious that the beam radius ω_a has a significant influence on the SMF coupling efficiency according to equation (4). We cannot change the beam spot radius precisely in the laboratory experiment system, so we just analyze the influence by theoretical simulation and the results are shown in Fig. 13. The nutation amplitude is 1 μm, and the coordinate of SMF core is (1 μm, 1 μm). The radius radio of beam and fiber are 1.5, 1.7, 1.9 and 2.2, respectively. We can obtain that, as the radius radio increases, the maximum coupling efficiency first increases and then decreases sharply. The best coupling efficiency can be achieved when the radio is 1.7. This indicates that the radius of the focus lens must be under consideration to ensure an appropriate Airy disk size.

5.3 The Influence of Nutation Amplitude

Fig. 14 shows that the coupling efficiency curves with different nutation amplitudes in the fine scanning stage. The offset and the coordinate are the same as the parameters mentioned above. It can be seen that, as the amplitude increases, the difference between the minimum and maximum values first increases and then decreases, as same as described in the literature [14]. The maximum difference of the purple line is about 0.46 which indicates the calculation accuracy of SMF core will be improved when the amplitude is 2.5 μm.

6. Conclusions

In order to reach optimum single mode fiber coupling efficiency for free space optical communication system, an efficient coupling method is needed. Considering that there will be a large radial offset bias between beam spot and SMF center, an adaptive coupling method based on coarse-fine laser nutation technique was presented in this paper. A laboratory experiment system was established, and then the adaptive coupling was realized according to the proposed strategy and algorithm. The SMF center calculation accuracy of coarse and fine scanning stage were 0.25 μm and 0.01 μm, respectively. The average coupling efficiency of the system can increase from 0.351 in open loop under a simulated atmospheric turbulence to 0.6244 in closed loop, the corresponding average errors of coupling efficiency, coordinate calculation and offset compensation were 0.0356, (0.08803 μm, 0.08805 μm), 0.1245 μm, respectively. Finally, some factors which influence the system were analyzed theoretically, and the simulated results show that the aberration impacts the system performance most seriously which must be eliminated.

References

[1] G. Zheng, F. Zhou, J. Liu, T. Li, N. An, and B. Zhang, "Influence of temperature on divergence angle of a focal telescope used in laser optical communication," *Opt. Express*, vol. 20. no. 12, pp. 13208–13214, 2012.

[2] B. Li, S. Tong, L. Zhang, and Y. Liu, "Influence of horizontal atmospheric visibility on deep-space laser communication rate," *Acta Optica Sinica*, vol. 37, no. 10, 2017, Art. no. 1006003.

[3] A. J. Hashmi, A. A. Eftekhar, A. Adibi, and F. Amoozegar, "Analysis of telescope array receivers for deep-space inter planetary optical communication link between Earth and Mars," *Opt. Commun.*, vol. 28, no. 3, pp. 2032–2042, 2010.

[4] X. Sun, D. R. Skillman, E. D. Hoffman, and D. Mao, "Free space laser communication experiments from earth to the lunar reconnaissance orbiter in lunar orbit," *Opt. Express*, vol. 21, no. 2, pp. 1865–1871, 2013.

[5] M. R. Bell and S.-M. Tseng, "Capacity of the low-photon-rate direct-detection optical pulse-position-modulation channel in the presence of noise photons," *Appl. Opt.*, vol. 39, no. 11, pp. 1776–1782, 2010.

[6] J. Ma, L. Ma, Y. Qingbo, and Q. Ran, "Statistical model of the efficiency for spatial light coupling into a single-mode fiber in the presence of atmospheric turbulence," *Appl. Opt.*, vol. 54, no. 31, pp. 9287–9293, 2015.

[7] L. Tan, M. Li, Q. Yang, and J. Ma, "Fiber-coupling efficiency of Gaussian Schell model for optical communication through atmospheric turbulence," *Appl. Opt.*, vol. 54, no. 9, pp. 2318–2325, 2015.

[8] C. Zhai, L. Tan, S. Yu, and J. Ma, "Fiber coupling efficiency for a Gaussian-beam wave propagation through non-Kolmogorov turbulence," *Opt. Express*, vol. 23, no. 12, pp. 15242–15255, 2015.

[9] E. A. Swanson and R. S. Bondurant, "Using fiber optics to simplify free-space lasercom systems," in *Proc. Soc. Photo-Opt. Instrum. Free-Space Laser Commun. Technol. II*, 1990, vol. 1218, pp. 70–82.

[10] T. Weyrauch, M. A. Vorontsov, J. Gowens, and T. G. Bifano, "Fiber coupling with adaptive optics for free-space optical communication," *Proc. SPIE*, vol. 4489, pp. 177–184, 2002.

[11] H. Gao, H. Yang, and J. Xiang, "Auto-coupling method for making space light into single-mode fiber, optoelectronic Engineering," vol. 34, no. 8, pp. 126–129, 2007.

[12] H. Takenaka, M. Toyoshima, and Y. Takayama, "Experimental verification of fiber-coupling efficiency for satellite-to-ground atmospheric laser downlinks," *Opt. Express*, vol. 20, no. 14, pp. 15301–15308, 2012.

[13] W. Luo *et al.*, "Experimental demonstration of single-mode fiber coupling using adaptive fiber coupler," *Chin. Phys. B*, vol. 23, no. 1, 2014, Art. no. 014207.

[14] J. Gao, J. Sun, J. Li, R. Zhu, P. Hou, and W. Chen, "Coupling method for making space light into single-mode fiber based on laser nutation," *Acta Optica Sin.*, vol. 43, no. 8, 2016, Art. no. 0801001.

[15] H. He, J. Sun, and Y. Zhou, "Fine track system of space coherent optical communication without position detector," *Proc. SPIE*, vol. 1048, 2017, Art. no. 104816.

[16] M. Toyoshima, "Maximum fiber coupling efficiency and optimum beam size in the presence of random angular jitter for free-space laser systems and their applications," *J. Opt. Soc. Amer. A*, vol. 23, no. 9, pp. 2246–2250, 2006.

[17] C. Ruilier, "A study of degraded light coupling into single-mode fibers," *Proc. SPIE*, vol. 3350, pp. 319–329, 2007.

[18] F. Zhao, S. Yu, J. Ma, and L. Tan, "Orthonormal polynomials in analysis of single-mode fiber coupling," *Opt. Commun.*, vol. 28, no. 4, pp. 207–214, 2011.